

Adsorption of carbon dioxide onto PDA-CP-MS41 adsorbent

Kyu-Suk Hwang*, Lina Han*, Dae-Won Park*, Kwang-Joong Oh*,
Seong-Soo Kim**, and Sang-Wook Park*[†]

*Division of Chemical Engineering, Pusan National University, Busan 609-735, Korea

**School of Environmental Science, Catholic University of Pusan, Busan 609-757, Korea

(Received 11 May 2009 • accepted 11 June 2009)

Abstract—Carbon dioxide was adsorbed onto mesoporous adsorbent of PDA-CP-MS41, which was synthesized by CP-MS41 with propylene diamine, in a laboratory-scale packed-bed. Experiments were carried out at different adsorption temperatures (30-60 °C), amounts of adsorbent (1-3 g), and flow rates of nitrogen (15-60 cm³/min) to obtain the breakthrough curves of CO₂. These curves were tested by the deactivation model, which combined the adsorption of CO₂ and the deactivation of adsorbent particles. The adsorption rate constant and the deactivation rate constant were evaluated through analysis of the experimental breakthrough data using a nonlinear least squares technique. The experimental breakthrough data were fitted very well to the deactivation model than the adsorption isotherm models in the literature.

Key words: Adsorption, Carbon Dioxide, Breakthrough Curve, Deactivation Model, Mesoporous Adsorbent

INTRODUCTION

Carbon dioxide (CO₂) produced by the combustion of fossil fuels is regarded as the most significant greenhouse gas with its increasing accumulation in the atmosphere and has attracted worldwide attention [1]. Various methods have been used to remove it: absorption by solvent and adsorption by molecular sieve, membrane separation, and cryogenic fractionation. In particular, absorption has been widely used in the chemical industries, as with the Benfield Process [2]. Another technique is dry scrubbing or sorption of CO₂ onto an alkaline metal carbonate as a solid adsorbent. This is a modified hybrid technology of adsorption and chemical absorption, with the advantage of being a simple and convenient operation for separation and recovery of CO₂ in flue gases. The development of alkaline metal carbonates, such as an alumina gel [3], alumina [4], activated carbon [5-7], and silica/alumina vermiculite [8], is the focus of the current study to improve the sorption efficiency of the carbonate. Adsorption is one of the most widely employed methods in practical industrial operation because of the ease of operation and low cost with efficient recovery of the solute [9]. The most important characteristics of porous adsorbents are their surface properties such as porous structure, pore size distribution, wall thickness, specific surface area, and hydrophilic-hydrophobic properties. The discovery of the M41S family by a Mobil scientist [10,11] generated a great deal of interest in the synthesis of organically functionalized, mesoporous materials for their application in the fields of catalysis, sensing, and adsorption, given their high surface areas and large ordered pores ranging from 20 to 100 Å [11,12] with narrow size distributions. High chemical and thermal stabilities also make them potentially promising candidates for the reactions of bulky substrate molecules. In general, hybrid organic-inorganic materials have been prepared *via* post-grafting or co-condensation techniques. In 2000, Bhaumik and Tatsumi [13]

reported a grafting technique through a co-condensation method for hybrid MCM-41 using halogenated organosilanes. Recently, a new synthetic approach has been developed for the preparation of hybrid inorganic-organic mesoporous materials based on the co-condensation of siloxane and organosiloxane precursors in the presence of different templating surfactant solutions [14-17]. Huang and Yang [18] reported the sorption-reaction mechanism between CO₂ and a functional group of NH₂ attached in the adsorbent of 3-aminopropyltriethoxysilane - immobilized ionic liquid on MCM-46 and they presented the reaction of CO₂ onto the adsorbent. Xu et al. [19] used polyethyleneimine - immobilized adsorbent on MCM-41. Udayakumar et al. [20] reported a new grafting technique for the synthesis of hybrid MCM-41 and trialkylamine-immobilized ionic liquids containing high catalytic activity for the synthesis of cyclic carbonates from CO₂.

In mass transfer processes that accompany chemical reactions, such as a non-catalytic heterogeneous gas-solid reaction, the diffusion may have an effect on the reaction kinetics [21-26]. It is difficult and tedious to analyze the adsorption breakthrough curve using conventional isotherm models [27,28], such as the Langmuir, Freundlich, Brunauer-Emmett-Teller (BET), and Dubinin-Radushkevich-Kaganer (DRK) models, and prepare the experimental values of the sorption isotherm with a reasonable diffusivity [29] of a solute. Conversely, the deactivation model (DM) [30,31], as a simplified model, has been used to predict the breakthrough curve, assuming that the formation of a dense product layer over the surface of the adsorbent changed the number of active sites and the possible variations in the adsorption of active sites to cause a drop in the adsorption rate. Suyadal et al. [32] presented adsorption kinetics of trichloroethylene vapor on activated carbon using breakthrough curves by DM and assumed that the adsorption kinetics of DM were first-order with respect to organic vapor and zeroth order with respect to activity of the adsorbent, respectively. Park et al. have successfully applied DM for carbonation of sodium carbonate [33], potassium carbonate [34] with CO₂, adsorption of toluene vapor onto activated carbon

[†]To whom correspondence should be addressed.

E-mail: swpark@pusan.ac.kr

[35], and carbonation of rubidium carbonate [36]. They have indicated DM described gas-solid non-catalytic reactions more accurately than the unreacted core and volume reaction models, using deactivation kinetics with first-order with respect to the solid carbonate and the CO₂ concentration, respectively.

In this study, which is one of a series of works [33-36], the solid particle of PDA-CP-MS41 was selected as an adsorbent of CO₂. It was synthesized using CP-MS41 immobilized with propylene diamine in the previous work [20]. The experimental breakthrough data of CO₂ were used to obtain the adsorption kinetics in the deactivation model and to present the relationship between the breakthrough data and the adsorption isotherm.

THEORY

The formation of a dense product layer over the solid adsorbent creates an additional diffusion resistance and is expected to cause a drop in the adsorption rate. One would also expect it to cause significant changes in the accessible pore volume, active surface area, and activity per unit area of solid adsorbent with respect to the extent of the adsorption. All of these changes cause a decrease of vacant surface area of the adsorbent with time. In DM, the effects of all of these factors on the diminishing rate of CO₂ capture are combined in a deactivation rate term.

With assumptions [33] of the pseudo-steady state and the isothermal species, the conservation equation for CO₂ in the fixed bed is

$$-Q_o \frac{dC_d}{dS} - k_o C_d \alpha = 0 \quad (1)$$

In writing this equation, axial dispersion in the fixed bed and any mass transfer resistances are assumed to be negligible. According to the proposed DM, the rate of change of the activity of the solid adsorbent is expressed as

$$-\frac{d\alpha}{dt} = k_d C_d^n \alpha^m \quad (2)$$

The zeroth solution of the deactivation models is obtained by taking $n=0$, $m=1$, and the initial activity of the solid as unity.

$$a = \exp[-k_o \tau \exp(-k_d t)] \quad (3)$$

Eq. (3), which is identical to the breakthrough equation proposed by Suyadal et al. [32], assumes a fluid phase concentration that is independent of deactivation processes along the adsorber. More realistically, one would expect the deactivation rate to be concentration-dependent and, accordingly, axial-position-dependent in the fixed bed.

To obtain the analytical solution of Eq. (1) and (2) by taking $n=0$, $m=1$, an iterative procedure is applied. The procedure used here is similar to the paper proposed by Dogu [37] for the approximate solution of nonlinear equations. In this paper, the zeroth solution of Eq. (3) is substituted into Eq. (2), and the first correction for the activity is obtained by the integration of this equation. Then, the corrected activity expression is substituted into Eq. (1), and integration of this equation gives the first corrected solution for the breakthrough curve.

$$a = \exp \left[\frac{[1 - \exp(k_o \tau (1 - \exp(-k_d t)))]}{1 - \exp(-k_d t)} \exp(-k_d t) \right] \quad (4)$$

This iterative procedure can be repeated for further improvement of the solution. In this procedure, higher-order terms in the series solutions of the integrals are neglected. The breakthrough curve for the deactivation model with two parameters (k_o , τ and k_d) is calculated from the concentration profiles by Eq. (4).

EXPERIMENTAL

1. Chemicals

All chemicals were of reagent grade and were used without further purification. Purity of both CO₂ and N₂ was greater than 99.9%. Propylene diamine (PDA), tetraethylorthosilicate (TEOS), 3-chloropropyltriethoxysilane (CITPES), cetyltrimethylammonium bromide (CTMABr), and tetramethylammonium hydroxide were supplied by Aldrich chemical company, U.S.A.

2. Synthesis of PDA-CP-MS41

CP-MS41 was synthesized by hydrolysis of TEOS, as a silicon source, with CITPES as an organosilane using CTMABr as a template. PDA-CP-MS41 was synthesized by immobilization of PDA on the mesoporous CP-MS41. Both synthetic procedures of CP-MS41 and PDA-CP-MS41 followed previous work [20]. The surface area and size of CP-MS41 were measured by BET isotherm and SEM, and their values were 884.6 m²/g and 5.0 μm, respectively.

3. An Apparatus for CO₂ Capture and its Operation

An adsorption experiment (Fig. 1) was carried out in the presence of CO₂ with PDA-CP-MS41 adsorbent in a fixed bed Pyrex glass reactor with internal diameter of 2 cm. CO₂ was carried by nitrogen gas through a sparger. The concentration of CO₂ in the nitrogen stream at the outlet of the sparger was measured by a gas chromatograph. The flow rate of gas mixture of CO₂ and nitrogen was within the range of 15-60 cm³/min (measured at 25 °C). The amount of adsorbent and the adsorption temperature were in the range of 1-3 g, 30-60 °C, respectively. Each experiment was duplicated at least once under identical conditions. A gas chromatograph (detector: thermal conductivity detector; column: Haysep D (10 feet by 1/8 inch of stainless steel; detector temperature: 190 °C; feed temperature: 160 °C; flow rate of He: 25.7 cm³/min; retention time of N₂, CO₂: 1.497, 2.08 min, respectively.) connected to the exit stream of the adsorber allowed for on-line analysis of CO₂ and N₂.

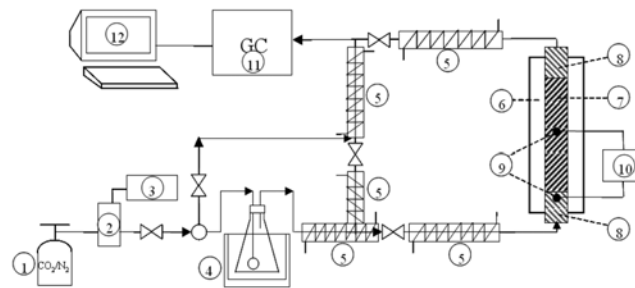


Fig. 1. Schematic diagram of a fixed bed apparatus.

- | | |
|-------------------------|-----------------------------|
| 1. Gas bomb | 7. Sample |
| 2. Mass flow controller | 8. Glass wool |
| 3. Flow indicator | 9. Temperature probe |
| 4. Saturator | 10. Temperature controller |
| 5. Heating line | 11. GC (gas chromatography) |
| 6. Furnace | 12. Personal computer |

PDA-CP-MS41 particles were supported by glass wool from both sides. The adsorber was placed into a tubular furnace equipped with a temperature controller. The length of the fixed adsorbent section of the bed was 5 cm of the adsorber. Temperature profiles were not observed within this section. All of the flow lines between the adsorber and the gas analyzer were heated to eliminate any condensation. Three-way valves placed before and after the adsorber allowed for flow of the gaseous mixture through the bypass line during flow rate adjustments. Composition of the inlet stream was checked by the analysis of the stream flowing through the bypass line at the start experiments. The adsorptions of CO_2 with and without moisture were carried out through the sparger and bypass without the sparger, respectively. The apparatus and experimental procedure used to obtain the breakthrough curve of CO_2 were identical with those in the previous work [36].

RESULTS AND DISCUSSION

1. Adsorption Accompanied with Chemical Reaction

Huang and Yang [18] and Leal et al. [38] presented the chemical reaction mechanism between CO_2 and the amine-immobilized-MCM48 and amine-immobilized-3-aminopropyltriethoxysilane, respectively, where the adsorption of CO_2 onto the solid particles with and without moisture was as follows:

They presented FTIR such as $-\text{NHCOO}^-$ and $-\text{NH}_3^+$ at $1,411\text{ cm}^{-1}$ (carbamate) without moisture and $-\text{N}^+\text{H}_3-\text{HCO}_3^-$ at $1,411\text{ cm}^{-1}$ (bicarbonate) with moisture, formed by the reaction CO_2 and $-\text{NH}_2$. Also, from TGA analysis, the presence of water moisture doubled the amount of CO_2 adsorbed.

In this study, the surface interaction of CO_2 with PDA-CP-MS41 was studied by infrared spectroscopy. Strong IR bands were observed in the range of $1,700\text{--}1,300\text{ cm}^{-1}$; adsorbed gaseous CO_2 , carbamate in C-O bending and NH_3^+ without moisture, bicarbonate

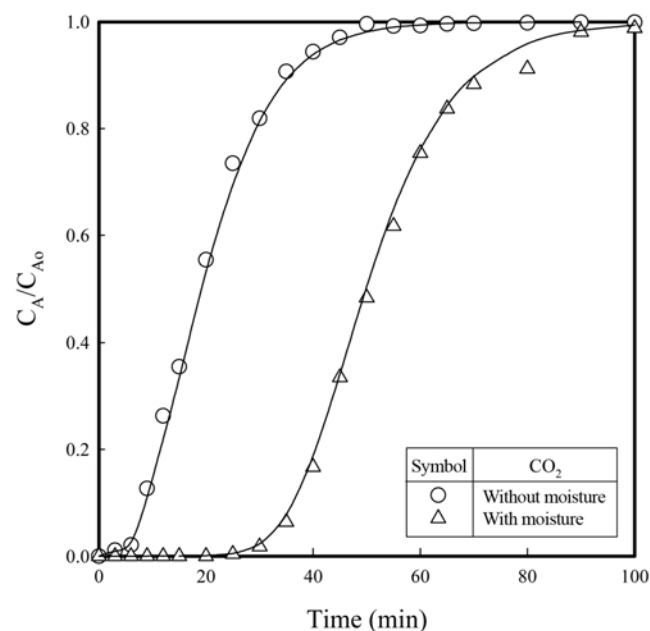


Fig. 2. Effect of moisture on the breakthrough curve of CO_2 ($Q_0 = 35\text{ cm}^3/\text{min}$, $y_A = 0.15$, $W = 2\text{ g}$, $T = 30\text{ }^\circ\text{C}$).

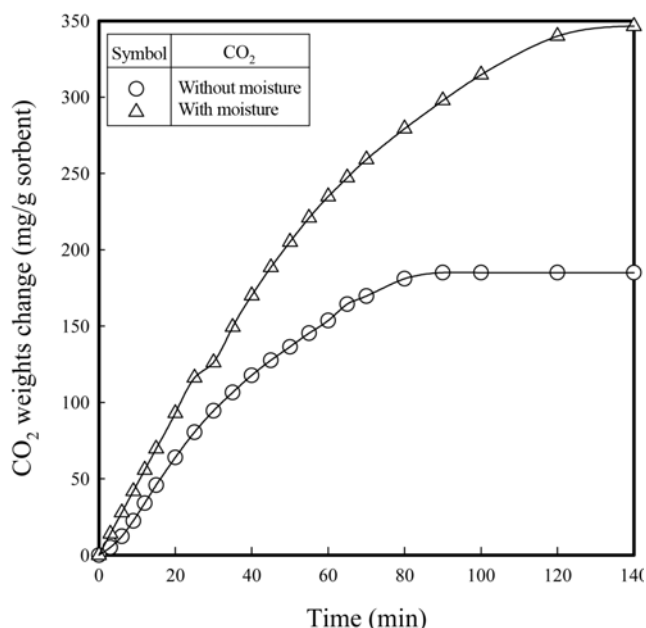


Fig. 3. Amount of CO_2 adsorbed with/without moisture under the same experimental conditions in Fig. 2.

in C-O bending with moisture. These IR bands coincided with those [18,38] mentioned above.

The breakthrough curves of CO_2 were measured under the typical conditions of CO_2 concentration of 15%, the flow rate of the gaseous mixture of $35\text{ cm}^3/\text{min}$, temperature of $30\text{ }^\circ\text{C}$, and PDA-CP-MS41 of 2 g with and without moisture, and shown in Fig. 2-8.

As shown in Fig. 2, the breakthrough curve shifts toward the right with moisture. The parameters of $k_o\tau$ and k_d were evaluated by analysis of the experimental breakthrough data with DM using a nonlinear least squares technique and listed in Table 2. This $k_o\tau$ was larger than that without moisture and the k_d , smaller than that without moisture.

To evaluate the adsorbed amounts of CO_2 , the upper areas of the breakthrough curves of CO_2 in Fig. 2 were integrated according to the adsorption stream time and are shown in Fig. 3.

As shown in Fig. 3, the amount of CO_2 adsorbed with moisture was $346.52\text{ mg/g-adsorbent}$, which was 87.3% larger than $185.08\text{ mg/g-adsorbent}$ during 100 minutes. It might be experimental error that the adsorbed CO_2 was not double. The results in Fig. 3 coincide with those [18] mentioned above. The surface reaction mechanism of CO_2 without and with moisture in adsorption onto PDA-CP-MS41 is shown in Fig. 4 [38]. As shown there, CO_2 used surface amino propyl group to an ammonium carbamate species when moisture was absent and an ammonium bicarbonate species when moisture was incorporated into the system.

2. Kinetics of CO_2 Adsorption on PDA-CP-MS41

To investigate the adsorption kinetics of CO_2 on PDA-CP-MS41 using two parameters of DM, the breakthrough curves of CO_2 were measured according to changes of the experimental variables such as flow rate of carrier gas, amount of adsorbent, and adsorption temperature. The parameters of $k_o\tau$ and k_d in DM were evaluated by analysis of the experimental breakthrough data with DM using a nonlinear least squares technique, as mentioned in section 1.

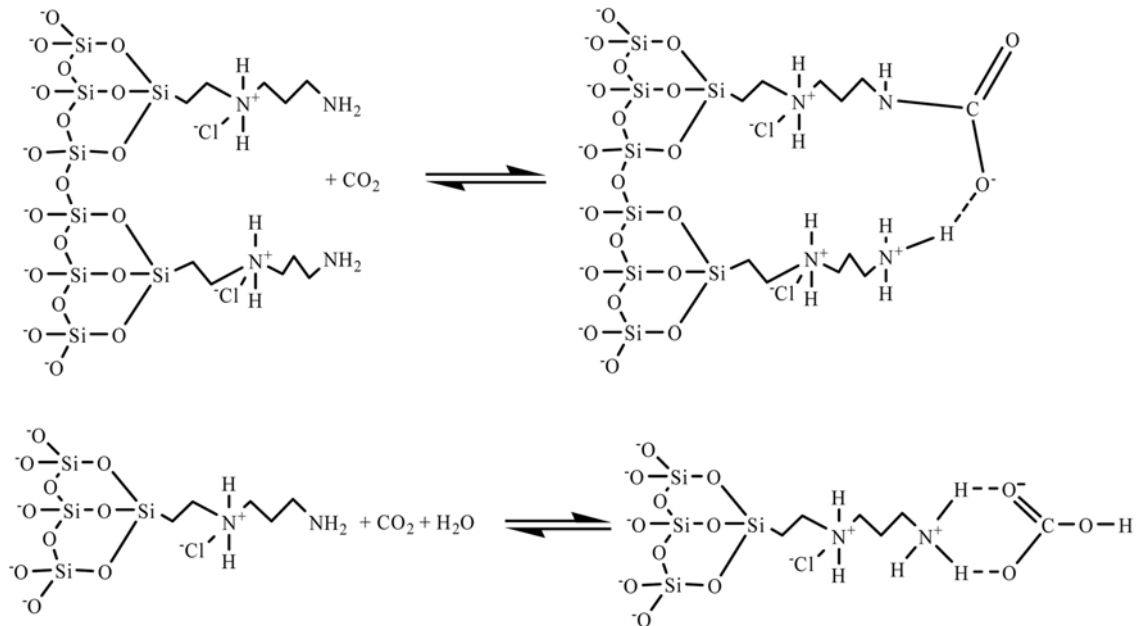


Fig. 4. Surface reaction mechanism of CO₂ without and with moisture for adsorption of CO₂ onto PDA-CP-MS41.

2-1. Effect of Flow Rate of Gaseous Mixtures of CO₂ and N₂

To investigate the effect of flow rate of gaseous mixtures of CO₂ and N₂ on the kinetics, the breakthrough curves of CO₂ were measured in the range of flow rate of gaseous mixtures from 15–60 cm³/min (measured at 25 °C) under the typical experimental conditions such as 15% of CO₂ concentration, 30 °C and 2 g of the adsorbent. The measured outlet concentrations of CO₂ were typically plotted against the adsorption time for the various flow rates indicated as various symbols in Fig. 5.

As shown in Fig. 5, a shift of breakthrough curves to shorter times

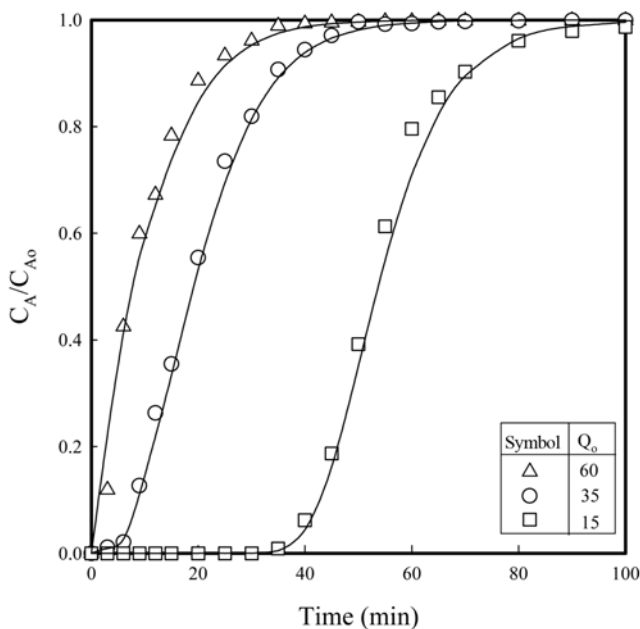


Fig. 5. Effect of flow rates of gaseous mixtures on the breakthrough curve of CO₂ ($y_A=0.15$, $W=2$ g; $T=30$ °C).

was observed at greater flow rate of the gaseous mixture with decrease in the amount of CO₂ that the bed can hold up to a certain breakthrough level. This result means that the adsorbed amount of CO₂ decreases as the space time of the gaseous mixtures in the fixed bed decreases. From analysis of the experimental breakthrough data, $k_o\tau$, k_o , and k_d were evaluated and tabulated in Table 1. As shown, the values of $k_o\tau$ decrease with increasing Q_0 , where the k_o 's and k_d 's are almost the same. The solid line in Fig. 5 was drawn with the calculated values of dimensionless concentration of CO₂ using $k_o\tau$ and k_d , and Eq. (4). As shown in Fig. 5, the regression of the experimental breakthrough data gave very good agreement with more than 99.7%.

2-2. Effect of Amount of PDA-CP-MS41

A set of experiments was performed to investigate the effect of the mass of PDA-CP-MS41 in the range from 1 to 3 g on the CO₂ breakthrough curves. As shown in Fig. 6, a good description of data was obtained by using Eq. (4) for each set of amount of PDA-CP-MS41 at y_A of 0.15, T of 30 °C, and Q_0 of 35 cm³/min. The parameters determined from the analysis of the experimental breakthrough data are tabulated in Table 1. As shown, the values of $k_o\tau$ increase with increasing W , whereas the k_o 's and k_d 's are almost same.

2-3. Effect of Feedstock Concentration of CO₂

To determine the dependence of the adsorption parameters on the feedstock concentration of CO₂, the breakthrough curves of CO₂ were measured in the range of CO₂ concentration from 5–50% at flow rate of the gaseous mixture of 35 cm³/min, temperature of 30 °C, and PDA-CP-MS41 of 2 g. A good fitting of DM predictions to experimental data could be seen by inserting the corresponding values of $k_o\tau$ and k_d tabulated in Table 1 into Eq. (4), which were almost same. The calculated breakthrough curve (solid line) of CO₂ with the mean values of $k_o\tau$ and k_d and measured ones (various symbols) are shown in Fig. 7. As shown in Fig. 4, the measured values approach the calculated value with a correlation coefficient of 0.9917 and mean deviation of 0.051. This result comes from independence

Table 1. Rate parameters for various experimental conditions

T (°C)	Q_o (cm ³ /min)	W (g)	y_A (-)	$k_o \tau$ (-)	$k_o \times 10^8$ (m/min)	k_d (m ³ /kmol · min)	r^2 (-)
30	15	2	0.15	5.716	4.836	0.113	0.997
30	35	2	0.15	2.207	4.357	0.121	0.996
30	35	2	0.15	4.365*	8.618*	0.094*	0.997
30	60	2	0.15	1.205	4.078	0.129	0.995
30	35	1	0.15	1.168	4.611	1.127	0.994
30	35	2	0.15	2.207	4.357	0.121	0.999
30	35	3	0.15	3.117	4.103	0.115	0.996
30	35	2	0.05	2.326	4.592	0.138	0.998
30	35	2	0.15	2.207	4.357	0.121	0.999
30	35	2	0.50	2.088	4.122	0.104	0.994
30	35	2	0.15	2.207	4.357	0.121	0.999
40	35	2	0.15	2.854	5.635	0.504	0.998
50	35	2	0.15	3.632	7.170	1.494	0.998
60	35	2	0.15	4.554	8.991	4.114	0.933

The asterisk symbol (*) means adsorption with moisture

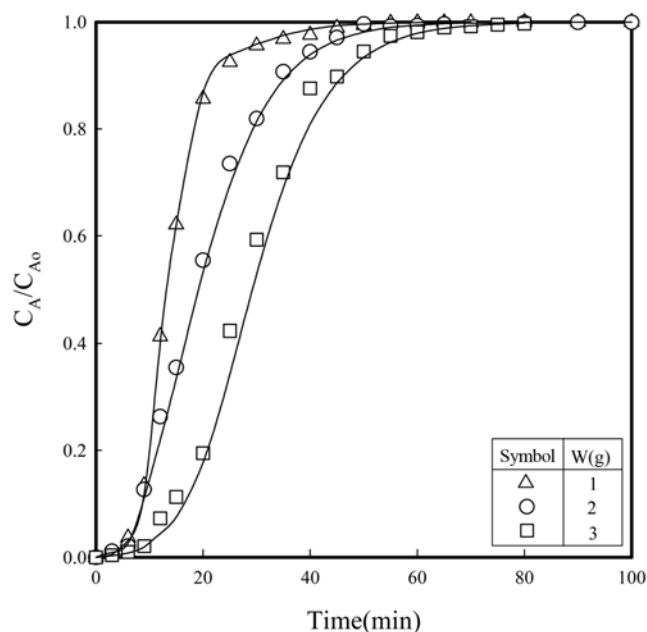


Fig. 6. Effect of amount of adsorbent on the breakthrough curve of CO₂ ($Q_o=35$ cm³/min, $y_A=0.15$, $T=30$ °C).

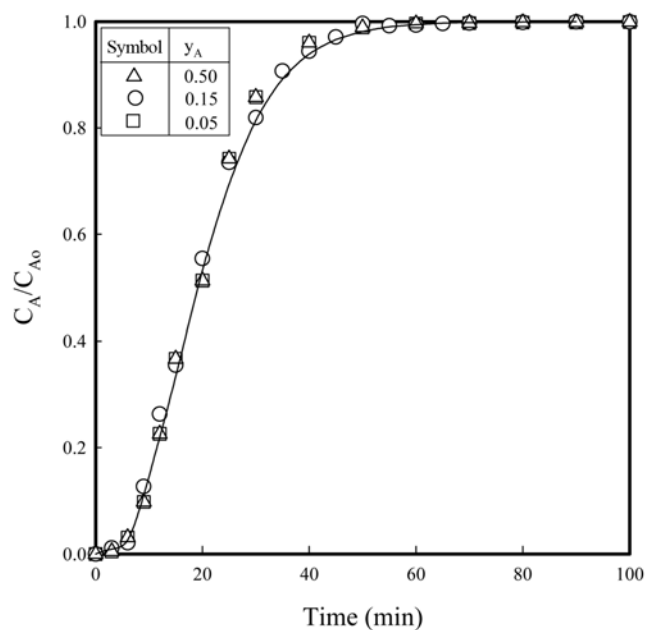


Fig. 7. Effect of CO₂ concentration on the breakthrough curve of CO₂ ($Q_o=35$ cm³/min, $W=2$ g, $T=30$ °C).

of the concentration of CO₂ on the breakthrough curves of CO₂ as shown in Eq. (4).

2-4. Effect of Adsorption Temperature

To investigate the effect of adsorption temperature on the adsorption kinetics, the breakthrough curves of CO₂ were measured in the range of temperature from 30–60 °C. The measured outlet concentrations of CO₂ were typically plotted against the adsorption time for the various temperatures indicated as various symbols in Fig. 8 under the typical experimental conditions of 35 m³/min of the gaseous mixture and 2 g of PDA-CP-MS41. The parameters are tabulated in Table 1. Fig. 8 indicates a shift in breakthrough curves toward the left with increased temperature, which might be attributed to an increase in the amount of adsorbed CO₂ due to increase of reaction

and deactivation and is the same result of the breakthrough curves of trichloroethylene vapor on EDA-CP-MS41 [32]. Arrhenius plots of k_o and k_d are shown in Fig. 9. The activation energy for the adsorption (ΔE_a) and deactivation (ΔE_d) were obtained from the slopes of plots in Fig. 6, and their values were 20.2 and 98.0 kJ/mole, respectively.

3. Comparison of the Proposed Models

Several equilibrium models [28], which have been developed to describe adsorption isotherm relationships, are useful for describing adsorption capacity and theoretical evaluation of thermodynamic parameters, such as heats of adsorption. But, sometimes the experimental procedure to prepare the adsorption isotherm relationships is very tedious and takes too much time. The equilibrium concentrations between two phases, which are used to describe adsorption

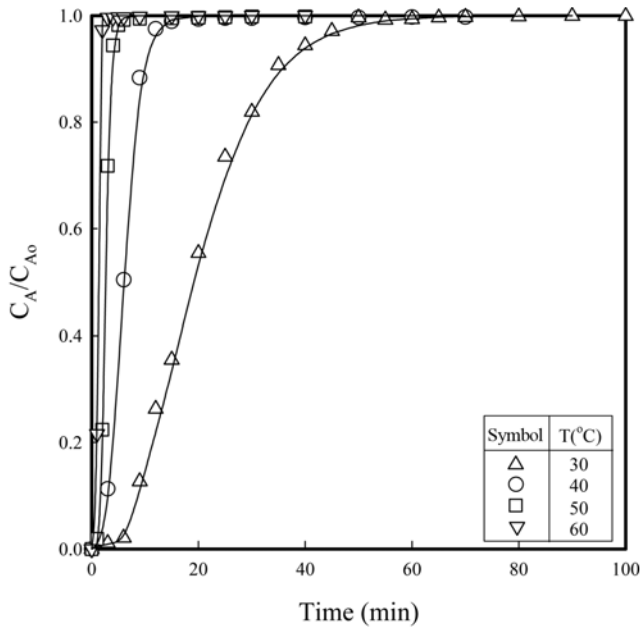


Fig. 8. Effect of CO₂ concentration on the breakthrough curve of CO₂ (Q₀=35 cm³/min, W=2 g, T=30 °C).

isotherm relationships, can be obtained by Eq. (5) and (6), where a(t), x and y are the dimensionless concentrations of CO₂ in the breakthrough data [39], in the gas phase and solid phase, respectively.

$$x = \frac{\int_0^t a(t) dt}{\int_0^\infty a(t) dt} \tag{5}$$

$$y = \frac{t - x \int_0^\infty a(t) dt}{\int_0^\infty dt - x \int_0^\infty a(t) dt} \tag{6}$$

As shown in Eqs. (5) and (6), the ranges of x and y are between 0

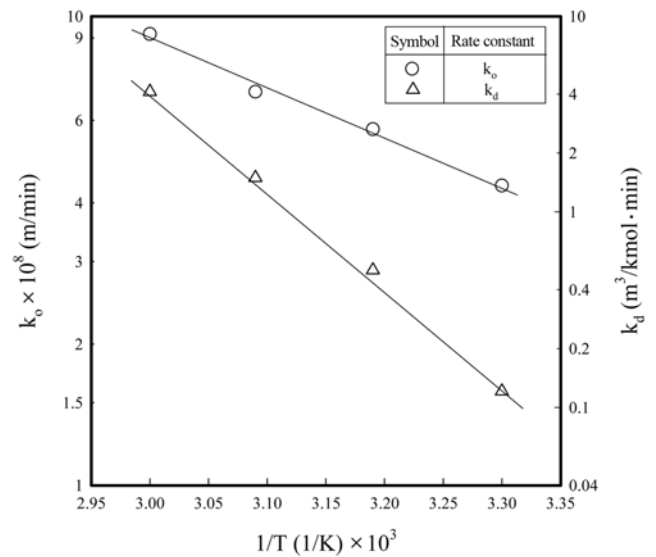


Fig. 9. Effect of adsorption temperature on dimensionless adsorption rate constant and deactivation rate constant.

and 1, respectively. The equilibriums for single-solute sorption given in the literature [28] are frequently presented as dimensionless concentration isotherms. To compare the deactivation model with the equilibrium isotherm models, models selected by Suyadal et al. [32] were used as follows: Langmuir, Freundlich, BET, and DRK model, whose formulas are listed in Table 2. The typical experimental conditions indicated as circle were used, i.e., gaseous flow rate of 35 cm³/min, amounts of PDA-CP-MS41, 2 g, and adsorption temperature, 30 °C. Using a(t) obtained from the experimental parameters, the values of x and y obtained from Eq. (5) and (6), were shown in Fig. 10 and used to obtain to give the constants of a and b in each model.

As shown in Table 2 and Fig. 10, the proposed deactivation model fitted the data with the highest correlation (r²) of 0.996, and the ad-

Table 2. Selected adsorption isotherms to fit the breakthrough data of CO₂ for comparison with the deactivation model

Adsorption isotherms	Mathematical representation of adsorption isotherms	Linearized forms	Parameters and correlation coefficient
Langmuir	$y = \frac{ax}{(1+bx)}$	$\frac{1}{y} = \frac{1}{ax} + \frac{b}{a}$	a=11.56 b=12.82 r ² =0.970
Freundlich	$y = ax^b$	$\ln(y) = \ln(a) + b \ln(x)$	A=1.0976 b=0.4466 r ² =0.977
Brunauer-Emmett-Teller	$y = \frac{x}{(1-x)(a+bx)}$	$\frac{x}{y(1-x)} = a + bx$	a=-1.0123 b=7.9187 r ² =0.680
Dubinin-Radshkevich-Kagener	$y = a \exp[-b \ln^2(x)]$	$\ln(y) = \ln(a) - b \ln^2(x)$	a=0.8480 b=0.1005 r ² =0.975
Deactivation model (this study)	x According to Eq. (5) y According to Eq. (6)		k _s τ=2.207 k _d =0.121 r ² =0.996

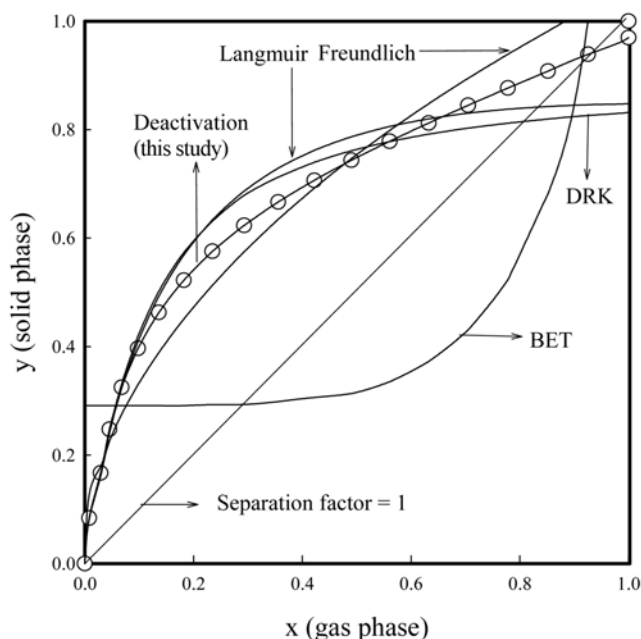


Fig. 10. Comparison of the model in describing the experimental breakthrough curve of CO₂ according to Table 2 under the same experimental conditions in Fig. 8.

sorption of CO₂ on PDA-CP-MS41 might be favorable isotherms due to the separation factor less than unity. Failure of BET, Langmuir, DRK, and Freundlich model in order in the fitting with the experimental data in Fig. 10 may be explained by the gas-solid heterogeneous reaction containing adsorption between CO₂ and PDA-CP-MS41.

CONCLUSIONS

Mesoporous PDA-CP-MS41 was used as an adsorbent to capture CO₂, and the breakthrough data were measured in a fixed bed to observe the adsorption kinetics. The adsorption kinetics was assumed to be the first-order with respect to the concentration of CO₂ and the activity of the adsorbent, respectively. The adsorption and deactivation rate constant were evaluated by the deactivation model through analysis of the experimental breakthrough data by using a nonlinear least squares technique. Moisture actually increased the CO₂ adsorption capacity because of the special chemical reaction mechanism between CO₂ and amines in PDA-CP-MS41. The experimental breakthrough data were fitted very well to the deactivation model than the adsorption isotherm models in the literature.

NOMENCLATURE

a : ratio of outlet concentration of CO₂ to inlet concentration
 C_A : concentration of CO₂ in gaseous stream
 k_d : deactivation rate constant [m³/kmol·min]
 k_o : adsorption rate constant [m/min]
 m : deactivation order in Eq. (2)
 n : adsorption order in Eq. (2)
 Q_o : flow rate of gaseous mixtures of N₂ and CO₂ [m³/min]
 r² : correlation coefficient

S : surface area of adsorbent [m²]
 t : adsorption time [min]
 T : adsorption temperature [K]
 V_G : volume of gas in the absorber [m³]
 y_A : mole fraction of CO₂
 W : amount of adsorbent [g]

Greek Letters

α : activity of the solid adsorbent
 τ : surface-time defined as ratio of S to Q_o [min/m]

Subscripts

A : CO₂
 o : inlet

ACKNOWLEDGMENTS

This work was supported by Brain Korea 21 Project and a grant (2006-C-CD-11-P-03-0-000-2007) from the Energy Technology R&D of Korea Energy Management Corporation. Dae-Won Park is also thankful for KOSEF (R01-2007-000-10183-0).

REFERENCES

1. M. Aresta, *Carbon dioxide recovery and utilization*, Kluwer academic Pub., Boston (2003).
2. R. K. Bartoo, *Chem. Eng. Prog.*, **80**, 35 (1984).
3. W. Fuchs and N. T. Syosett, U. S. Patent 3,511,595 (1970).
4. D. Gidaspow and M. Onischak, U. S. Patent 3,865,924 (1975).
5. S. Hirano, N. Shigomoto, S. Yamada and H. Hayashi, *Bull. Chem. Soc. Jpn.*, **68**, 1030 (1995).
6. H. Hayashi, H. J. Taniuchi, N. Furuyashiki, S. Sugiyama, S. Hirano, N. Shigemoto and T. Nonaka, *Ind. Eng. Chem. Res.*, **37**, 185 (1998).
7. T. Shigemoto, S. Sugiyama and H. Hayashi, *J. Chem. Eng. Jpn.*, **38**, 711 (2005).
8. A. G. Okunev, V. E. Sharnov, Y. I. Aristov and V. N. Parmon, *React. Kinet. Catal. Lett.*, **71**, 355 (2004).
9. M. L. Ruhl, *Chem. Eng. Prog.*, **89**, 1344 (1993).
10. C. T. Kresge, M. E. Leonowicz, W. J. Roth, J. C. Vartuli, J. S. Beck, *Nature*, 359, **710** (1992).
11. J. S. Beck, J. C. Vartuli, W. J. Roth, M. E. Leonowicz, C. T. Kresge, K. D. Schmitt, C. T. W. Chu, D. H. Olson, E. W. Sheppard, S. B. McCullen, J. B. Higgins and J. L. Schlenker, *J. Am. Chem. Soc.*, **114**, 10834 (1992).
12. D. Zhao, J. Feng, Q. Huo, N. Melosh, G. H. Fredrickson, B. F. Chmelka and G. D. Stucky, *Science*, **279**, 548 (1998).
13. A. Bhaumik and T. Tatsumi, *J. Catal.*, **189**, 31 (2000).
14. S. L. Burkett, S. D. Sim and S. J. Mann, *J. Chem. Soc. Chem. Commun.*, 1367 (1996).
15. M. H. Lim, C. F. Blanford and A. Stein, *J. Am. Chem. Soc.*, **119**, 4090 (1997).
16. C. E. Fowler, B. Lebeau and S. Mann, *J. Chem. Soc. Chem. Commun.*, 1825 (1998).
17. F. Babonneau, L. Leite and S. Fontlupt, *J. Mater. Chem.*, **9**, 175 (1999).
18. H. Y. Huang and R. T. Yang, *Ind. Eng. Chem. Res.*, **42**, 2427 (2003).
19. X. Xu, C. Song, B. G. Miller and A. W. Scaroni, *Fuel Proc. Tech.*

- nol.*, **86**, 1457 (2005).
20. S. Udayakumar, S. W. Park, D. W. Park and B. S. Choi, *Catal. Commun.*, **9**, 1563 (2008).
 21. L. K. Doraiswamy and M. M. Sharma, *Heterogeneous reactions*, John Wiley & Sons, New York (1954).
 22. M. Ishida and C. Y. Wen, *AIChE J.*, **14**, 311 (1968).
 23. P. A. Pamachandran and B. D. Kulkarni, *Ind. Eng. Chem. Res. Process Des. Dev.*, **19**, 717 (1980).
 24. J. W. Evans and S. Song, *Ind. Eng. Chem. Process Des. Dev.*, **13**, 146 (1974).
 25. B. S. Sampath, P. A. Ramachandran and R. Hughes, *Chem. Eng. Sci.*, **30**, 135 (1975).
 26. M. G. Ranade and J. W. Evans, *Ind. Eng. Chem. Process Des. Dev.*, **19**, 118 (1980).
 27. D. M. Ruthven, *Principles of adsorption and adsorption processes*, John & Wiley, New York (1984).
 28. M. Suzuki, *Adsorption engineering*, Kodansha Ltd., Tokyo (1990).
 29. N. Orbey, G. Dogu and T. Dogu, *Can. J. Chem. Eng.*, **60**, 314 (1982).
 30. S. Yasyerli, T. Dogu, G. Dogu and I. Ar, *Chem. Eng. Sci.*, **51**, 2523 (1996).
 31. T. Kopac and S. Kocabas, *Chem. Eng. Comm.*, **190**, 1041 (2003).
 32. Y. Suyadal, M. Erol and M. Oguz, *Ind. Eng. Chem. Res.*, **39**, 724 (2000).
 33. S. W. Park, D. W. Sung, B. S. Choi and K. W. Oh, *Sep. Sci. Technol.*, **41**, 2665 (2006).
 34. S. W. Park, D. W. Sung, B. S. Choi, J. W. Lee and H. Kumazawa, *J. Ind. Eng. Chem.*, **12**, 522 (2006).
 35. S. W. Park, B. S. Choi and J. W. Lee, *Sep. Sci. Technol.*, **42**, 2221 (2007).
 36. K. S. Hwang, S. W. Park, D. W. Park, K. J. Oh and S. S. Kim, *Korean J. Chem. Eng.*, In Press.
 37. T. Dogu, *AIChE J.*, **32**, 849 (1986).
 38. O. Leal, C. Bolivar, C. Ovalles, J. J. Garcia and Y. Espidel, *Inorganica Chimica Acta*, **240**, 183 (1995).
 39. S. Yasyerli, G. Dogu and I. Ar, *Chem. Eng. Comm.*, **190**, 1055 (2003).